Journal of Engineering Science and Technology Review 15 (1) (2022) 154 - 161

JOURNAL OF
**Engineering Science and Technology Review**

www.jestr.org

Research Article

# Parameter Optimization and Microstructure Evolution of WC and BN Particle Reinforced Ni-based Composite Coating by Laser Cladding

**Ma Shibang[1*], Zheng Yue[2], Xu Yang[2], Wang Xing[1]**

[1]*School of Mechatronic Engineering, Nanyang Normal University, Nanyang 473061, China*
[2]*College of Engineering, China Agricultural University, Beijing 100083, China*

Received 29 December 2021; Accepted 15 April 2022

***Abstract***

Laser cladding is one of the most effective methods to improve the abrasion resistance and corrosion resistance of surfaces. Thus, it is widely used to reinforce steel surfaces. This study aimed to investigate the effects of laser parameters on the properties of the composite layer and the reinforcement of Ni-based composite powder on a steel surface by laser cladding. The laser cladding of Ni-based Ni60A + x%[WC (x%) + BN] composite powder on 45 steel surface to form WC + BN particle reinforced coating was evaluated by preplaced-powder method. The effects of laser power and scanning speed on mechanical property and hardness were assessed. Microstructure, phase composition, and energy spectrum were comprehensively analyzed by scanning electron microscopy, X-ray diffraction, and energy-dispersive spectrometry, respectively. Results reveal that the use of composite powder to form a reinforced coating on the 45 steel was feasible. At 24%[WC (80%) + BN] content, a cladding layer with a compact and homogeneous microstructure was obtained at 800 W laser power and 120 mm/min scanning speed. Numerous dispersedly distributed BN particles exist at the cladding layer, and the size and number of W compounds and BN particles gradually increased with increased WC + BN content. The findings of this study provide insights into the application and promotion of laser cladding on 45 steel materials.

*Keywords:* Laser cladding, Parameter optimization, Microstructure evolution, Reinforced WC + BN particles

## 1. Introduction

Wear damage is one of the main causes of steel part failure, especially under humid environment and high friction conditions [1]. The wear damage of steel parts mostly initiates on the surface. Various surface treatment technologies have been proposed for improving the performance of the matrix to prolong the service time of parts. Laser cladding is an advanced surface modification technology, in which high-energy laser beam is used to melt the surface of the substrate material and form a coating with a special function. This approach could fabricate high-performance surfaces with low-cost materials while reducing energy consumption and cost [2, 3, 4]. The material and process parameters are the main factors determining the performance of the cladding layer. At present, powder materials, such as metal, ceramic, and composite powders, are the most widely used cladding materials. Given its good wettability, corrosion resistance, wear resistance, self-lubrication effect, and moderate price, Ni-based self-melting alloy powder has been widely studied and applied [5, 6, 7]. WC particle has the characteristics of high hardness, corrosion resistance, and good thermal stability, and it is the main material for manufacturing cemented carbide and wear-resistant coating. Therefore, it is considered as a reinforced phase material for laser cladding composite and studied by many researchers [8, 9, 10]. BN particle has good self-lubricity, high thermal conductivity, good thermal stability, and corrosion resistance. It also has excellent metal mechanical properties and tribological properties of solid lubricant; thus, it can be used as an additive material in laser cladding processing [11, 12, 13]. The hardness of BN particles is not high, but from the perspective of the performance requirements of the coating, higher hardness is not better. The coating surface is required to have high wear resistance, and good friction reduction could better meet the special needs of some workpiece. BN particles are an excellent self-lubricating ceramic material [14], but they failed to attract extensive attention of scientific researchers because of their insufficient hardness and obvious advantages. Few literatures about exploring BN particle are available compared with WC, SiC, and other ceramic materials. Therefore, this study aimed to explore the influence of adding BN particle powder to the WC composite powder with known good mechanical properties in composite coating by laser cladding. It also aimed to explore the wear resistance of WC/BN-enhanced Ni-based composite coating.

This article aimed to use the preset of powder and orthogonal method to the process and structural properties of composite coating on steel surface by laser cladding. Ni60A was used as the bonding phase material, and WC and BN were used as raw materials in accordance with a certain ratio in the process of laser cladding. The main objective was to determine the appropriate reinforced elements and the best process parameters. The findings of this study could serve as a reference for the process optimization and application of WC/BN composite coating by laser cladding.

*E-mail address: mshibang@126.com
ISSN: 1791-2377 
doi:10.25103/jestr.151.19

## 2. State of the art

Many studies have investigated the laser cladding formed process. The carbides of W[15], Ti[16], Si[17], Cr[18], Zr[19], and B [20] and $SiO_2$ [21], $Al_2O_3$ [22], $ZrO_2$ [23], and other oxides are the main reinforced phases. Lu J. Z. et al. [24] investigated the various WC contents on H13 hot-working die steel to improve wear resistance. The results showed that WC particles play a strengthening role in the coatings, the un-melted WC particles in the coatings acted as a hard reinforcement, and their microhardness of Fe-based coatings were obviously improved. The coating with WC particles showed higher wear resistance and lower friction coefficient. B. AlMangour et al. [25] investigated the effects of applied laser energy density on the densification, microstructure, and mechanical properties of the selective laser melting processed parts, and they elucidated the mechanisms underlying the formation of TiC particles. The TiC reinforced phase exhibited good toughness, good lubricity, thermal and chemical stability, and good wear resistance. It significantly improved the hardness, compressive strength, and corrosion resistance of the composite coating. However, this study did not consider the effect of different power parameters on the coating performance. U.O. Okoli.et al. [26] cladded SiC powder on the surface of Ti-6Al-4V alloy to form surface metal matrix composite materials and improve the surface wear resistance by laser cladding. The SiC powder could serve as reinforcing particles, and it helped improve the surface wear properties in the resulting surface metal matrix composite. However, SiC wetted poor with the alloy pool, thus negatively affecting the quality of the surface. The wettability between the metal and reinforced SiC phases and the Ti-6Al-4V surface properties were improved by adding AL content. Zhang L. et al. [27] investigated the influence of laser power on the microstructure and properties of Co-based amorphous composite coatings produced by laser cladding on a 45 medium steel substrate. Their results demonstrated that as the laser power was increased, the average hardness of the cladding layer decreased, whereas the abrasion resistance increased. However, they did not evaluate the effect of laser scanning speed. Zhao Y. et al. [28] studied the microstructure and friction properties of Ni-based composite powder with the addition of h-BN lubricants (h-BN/Ni60) on Q235 steels by laser cladding. The results showed that the friction coefficient and wear rate of the Ni60A composite coating decreased with the addition of h-BN powder in a wide range of temperature of 25 °C–500 °C, but the hardness of the Ni60A composite coating decreased. Huang X. et al. [29] investigated the effects of WC and h-BN powder ratio on the microstructure and properties of Ni-based wear-resistant coatings on 45 steel by laser cladding. The results showed that the microstructure of the coating was improved, the mechanical properties of the tungsten carbide (WC)/Ni60 composite coating were optimized, the friction coefficient was reduced, the friction performance was improved, the residual stress at the interface was relieved, the friction coefficient decreased to approximately 0.1, the residual tensile stress at the interface decreased to 350 MPa, and the distribution of the residual stress was relatively gentle. However, the effect of specific process parameters of laser cladding on the microstructure and properties of the composite coating was not further studied.

The aforementioned works have mainly focused on the influence generated by WC reinforced phase and BN powder on the microstructure and properties of composite coating in laser cladding. However, the influence of laser power and scanning speed on the structure and properties of cladding layer has not been completely studied. The process parameters of composite coating with WC and BN powders as raw materials by laser cladding are rarely studied. In the present work, a 45 steel-based metal matrix composite layer was developed onto the 45 steel surfaces with Ni-based powder and WC and BN reinforced particles to improve the properties by laser cladding. The influence of laser power and scanning speed on the macroscopic quality, hardness, and microstructure of the cladding layer were studied. The optimized process parameters of the laser cladding were determined.

The remainder of this study is organized as follows. Section 3 describes the experimental materials and methods. Section 4 analyzes the effects of power and scanning speed on the macroscopic quality and hardness as well as, the microstructure. The conclusions are summarized in Section 5.

## 3. Methodology

In this work, 45 steel was chosen as the substrate material, Ni60A was used as the bonding phase, and WC and BN powders were used as the raw materials to generate reinforced phase by laser cladding. The 45 steel samples with gauge dimensions of $145mm \times 125mm \times 10mm$ were prepared by electro-discharge machining. The surfaces of these samples were sand blasted prior to laser processing to remove the oxide scale and then ultrasonically cleaned in alcohol to eliminate dirt and oil. Ni-based Ni60A + x%[WC (x%) + BN] composite powder with WC:BN = 4:1 (at.%) was used as the cladding material. The weight contents of WC (80%)+BN were set to 12%, 24%, 36%, 48%, and 60%. The Ni60A alloy powder size was −140 + 325 mesh, and its chemical composition is presented in Table 1. The composite powder was completely mixed and ground to guarantee homogeneity. In addition, 5% polyvinyl alcohol solution was used as the adhesive to bond the preplaced powder. After the preplaced powder was naturally dried, the TruDiod4006 semiconductor laser processing system was used to conduct the cladding experiment (Fig. 1).

**Table 1.** Chemical composition of Ni60A alloy powder

| Element | Cr | B | Si | C | Fe | Ni |
|---|---|---|---|---|---|---|
| Mass fraction/% | 17.0 | 3.5 | 4.0 | 1.0 | < 5.0 | Bal |

A 1-mm thick acrylic plate was used as an auxiliary coating tool to preplace the powder and ensure the thickness of the powder layer. The grooves with gauge dimensions of $40mm \times 5mm$ and $60mm \times 20mm$ on acrylic plate were milled with a laser cutting machine, and the preplaced powder layer was set to 1 mm. The preset of the cladding powder is shown in Fig. 2. Laser energy density $P_w$ ($W \cdot s \cdot mm^{-2}$) was introduced to examine the influence of laser power $P$ and scanning speed $v$ on the properties of the cladding layer.

The equations describing the relationships among the laser power $P$, the laser facula area $S$, and the scan speed $v$ are as follows:

$$P_w = Pt / S \tag{1}$$

$$t = 60D / v \tag{2}$$

$$S = \pi(D/2)^2 \tag{3}$$

The equation for the activation energy $P_w$ could be transformed from Eqs. (1)–(3) as follows:

$$P_w = 1.27 \cdot 60P / (D \cdot v) \tag{4}$$

where $D$ (mm) is the diameter of laser facula, $t(s)$ is the scanning time of the unit area, $S$ is the area of the laser facula, and $\pi$ is a constant (3.14). Orthogonal method was used, and the parameters of the laser cladding are shown in Table 2. The diameter of the laser facula was 3 mm, the voltage of defocus motor was 20 V, and the airflow speed coaxial protection of Ar gas protects was 20 mL/min. The post-laser cladding microstructure was characterized by scanning electron microscopy (SEM) with a Leica-S440i-SEM machine. Elemental analysis was conducted by energy disperse spectroscopy (EDS). Phase qualitative analysis was performed by X-ray diffraction (XRD) with a D/MAX2500-XRD machine. The hardness of the cladding layer was measured using a TMVP-1 Vickers Hardness Tester.

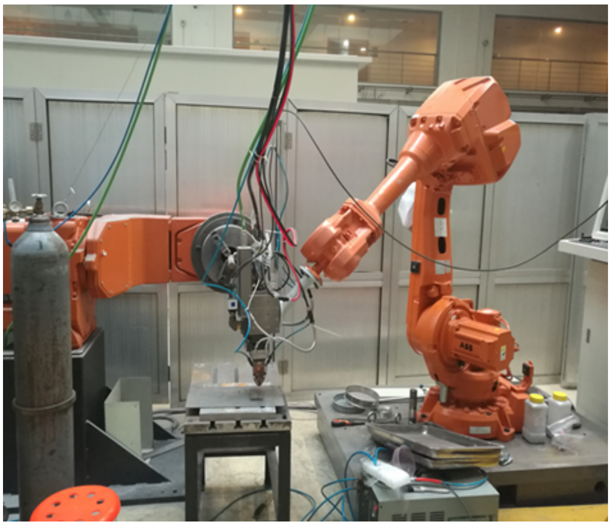

**Fig. 1.** Laser cladding system

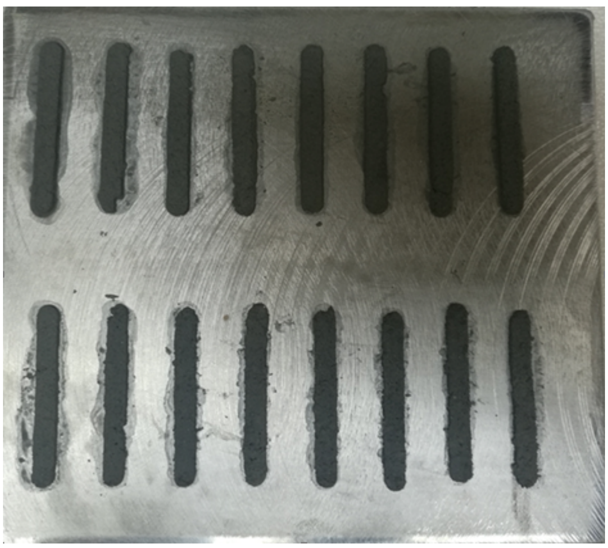

**Fig. 2.** Preset of the cladding powder

**Table 2.** Parameters of laser cladding of orthogonal test selection

| Coating No. | *P* (W) | *V* (mm/s) | *Pw* (kW·s·mm$^{-2}$) |
|---|---|---|---|
| A1 | 600 | 100 | 152.4 |
| A2 | 800 | 100 | 203.2 |
| A3 | 1000 | 100 | 254.0 |
| A4 | 1200 | 100 | 304.8 |
| A5 | 1400 | 100 | 355.6 |
| B1 | 600 | 120 | 127.0 |
| B2 | 800 | 120 | 169.3 |
| B3 | 1000 | 120 | 211.7 |
| B4 | 1200 | 120 | 254.0 |
| B5 | 1400 | 120 | 296.3 |
| C1 | 600 | 140 | 108.9 |
| C2 | 800 | 140 | 145.1 |
| C3 | 1000 | 140 | 181.4 |
| C4 | 1200 | 140 | 217.7 |
| C5 | 1400 | 140 | 254.0 |

## 4. Results analysis and discussion

### 4.1 Macroscopic morphology of the cladding layer

#### 4.1.1 Influence of laser power on the macrostructure

Fig. 3 shows the macrostructures of the cladding layer at different laser power values and a scanning speed of 100 mm/min. The surface of the coating was black, and it showed metallic luster after lightly polishing with sandpaper. This is the ash generated by the high-temperature vaporization combustion of organic binder, which is attached to the surface of the molten pool. The width of the coating gradually increased as the laser power was increased. At a low laser power of 600 W, the cladding layer was narrow and discontinuous. The width slightly increased at the laser power of 800 W. The cladding layer achieved an appropriate width and a smooth surface when the laser powers were 1000 and 1200 W. As the power reached 1400 W, the width of the cladding layer increased obviously, the groove became filled with the cladding layer, and the surface became over-burned. Thus, the optimal laser power was determined to be between 1000 and 1200 W.

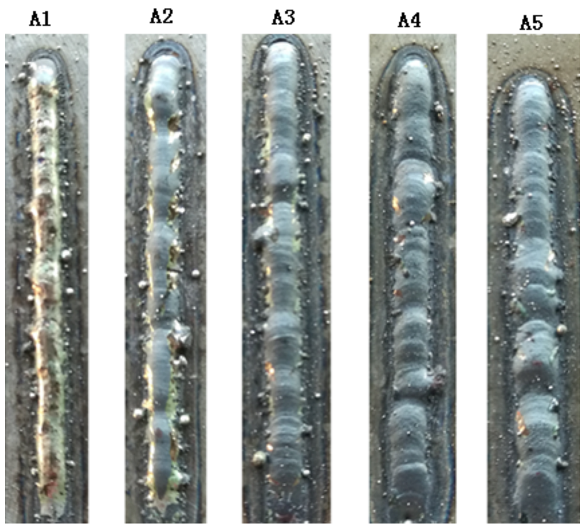


**Fig. 3.** Macro morphology of the cladding layer at different laser power values

#### 4.1.2 Influence of scanning speed on the macrostructure

Fig. 4 shows the macrostructures of the cladding layer at three different scanning speeds at the power of 1000 W. The width varied slightly, and the surface was smooth, indicating that the selected range of scanning speed was appropriate and that the effects of the different scanning speeds on the macrostructure were not evident.


**Fig. 4.** Macro morphology of the cladding layer at different scanning speeds

## 4.2 Hardness of the cladding layer

### 4.2.1 Influence of laser power on hardness

Fig. 5 shows the influence of laser power on the hardness of the cladding layer Ni60A + 24%[WC (80%) + BN]. At a constant scanning speed, the hardness increased first and then declined as the laser power continued to increase. The maximum hardness values were 885, 938, and 910 HV1 at the scanning speeds of 100, 120, and 140 mm/min, respectively.

The results indicated that laser power exerted an obvious effect on the hardness. At 600 W, the laser power was too low to completely melt the composite powder; thus, fine dendrites could not be formed, resulting in low hardness. As the power increased, carbide and fine dendrites appeared, and the hardness increased. Thus, the hardness reached the maximum value due to the optimal microstructure. Beyond that, the power was excessively high, such that the composite powder melted excessively, and the dendrite microstructures coarsened. Thus, the matrix element diluted to the cladding layer, leading to hardness reduction.

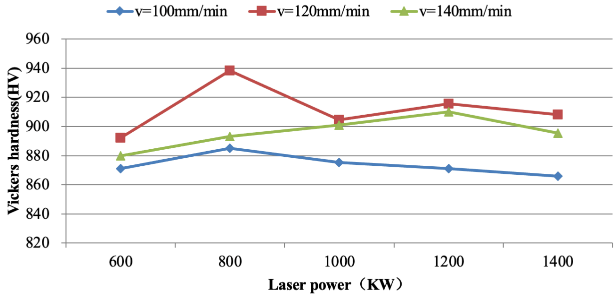


**Fig. 5.** Effect of laser power on the hardness of the cladding layer

### 4.2.2 Influence of scanning speed on hardness

Fig. 6 shows the influence of scanning speed on the hardness of the cladding layer Ni60A + 24%[WC (80%) + BN]. As shown, the effect was insignificant. At a constant laser power, the change tendency of the hardness increased with the increase in scanning speed, and after reaching the extreme value, it decreased with the increase in scanning speed. The maximum hardness values all appeared at the scanning speed of 120 mm/min. The maximum hardness values were 892.14, 938.43, 904.4, 915.67, and 908 HV1 at the laser powers of 600, 800, 1000, 1200, and 1400 W, respectively. The hardness test results showed that scanning speed has a remarkable effect on the hardness of cladding layer. The absorbed energy was negatively correlated with the scanning speed. The melting degree of the composite powder positively influenced the absorbed energy. The faster the scanning speed is, the less energy absorbed by the cladding layer and the lower the melting degree of the composite coating material. On the contrary, the slower the scanning speed is, the higher the melting degree of the composite coating material.

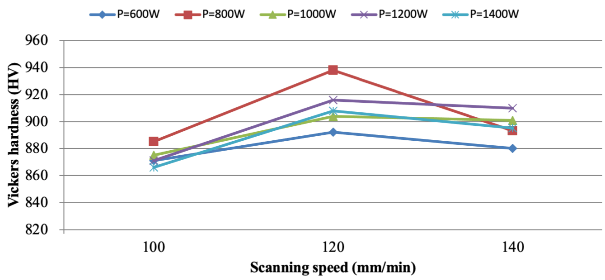


**Fig. 6.** Effect of scanning speed on the hardness of the cladding layer

## 4.3 Microstructure

### 4.3.1 Phase analysis of the cladding layer

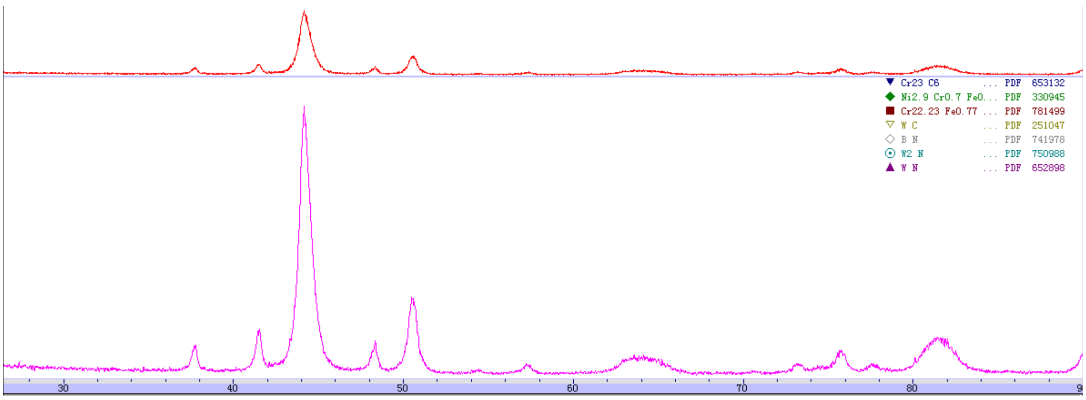


**Fig. 7.** XRD spectrum of the Ni60A + 24%[WC (80%) + BN] composite coating

Fig. 7 shows the XRD pattern of the coating of Ni60A + 24%[WC (80%) + BN] formed at the laser power of 1400 W and the scanning speed of 120 mm/min. The main phases were the solid solution of Ni-Cr-Fe, the compound of $Cr_{23}C_6$, the eutectic compound of $Cr_{22.23}Fe_{0.77}C_6$, and the reinforced-phase WC and BN. As the spectrum showed that the contents of WC and BN were close, the peak searching range was enlarged and WC mainly generated $Cr_4N_{15}W$, $Ni_{17}W_3$, $Fe_7W_6$, $W_2B$, and other phases. Phase retrieval results showed that WC and BN were successfully fused into the composite coating under the set processing parameters, indicating that the experiment approach is feasible by using WC + BN two-phase ceramic material as the reinforced phase and self-lubricating phase.

The diffraction peaks of Ni-Cr-Fe solid solution was the strongest, followed by $Cr_{23}C_6$. In the laser cladding process, the composite powder and the matrix surface were melted, and Fe was diluted to the cladding layer. The electronegativity and atomic radius of Ni, Fe, and Cr were similar. The face-centered cubic lattice structure consisted of γ-Fe and Ni. Thus, the γ-(Ni, Fe) solid solution and the intermetallic $Ni_{2.9}Cr_{0.7}Fe_{0.36}$ were easily formed under the melting condition. Phase retrieval revealed that the content of WC was low in the coating, implying that it was completely decomposed at high temperatures. Cr and C showed strong affinity, and Cr combined with the C generated by WC decomposition in the melting state, which is the reason for the second peak $Cr_{23}C_6$ in the coating spectrum. W demonstrated stable chemical properties after being separated, and not suitable elements were found to combine with it. Moreover, due to the similar electronegativity and atomic radius of Ni, Fe, and Cr, W formed the compounds $Cr_4N_{15}W$, $Ni_{17}W_3$, and $Fe_7W_6$ with Ni, Cr, and Fe. Furthermore, the laser cladding process is a non-equilibrium process of rapid solidification, and metastable and intermediate phases were formed. These phases are sensitive to the solidification condition and prone to the lattice distortion. Thus, a number of diffraction peaks that could not be matched was present.

### 4.3.2 Energy spectrum analysis of the cladding layer

The chemical composition of the microstructure was confirmed by energy spectrum analysis. As shown in Fig. 8, the microstructure of the Ni60A + 24%[WC (80%) + BN] cladding layer displayed three different phases: the dark gray phase was the dendritic structure, the off-white phase was the eutectic microstructure, and a small amount of black granular phase. The black granular phase was circular in shape and uniformly distributed. EDS was conducted on the three different phases, and the measured position is shown in Fig. 8.

The compositions of the different points are provided in Table 3. Fe was enriched at the cladding layer, demonstrating that an atomic diffusion occurred between the composite coating and the matrix. Such diffusion was beneficial for improving the bonding strength. Considerable amounts of Fe, Ni, and Cr existed at the matrix, suggesting that the main dendritic phase was the γ-(Ni,Fe) solid solution .The eutectic structure contained more Fe, W, B, and Cr, and the main phases of the eutectic structure were $Cr_{23}C_6$, $Ni_{2.9}Cr_{0.7}Fe_{0.36}$, $B_2Fe_3Ni_3$ and various W compounds. The content of N in particle phase was significantly more than the other positions. According to the uniqueness of the source of N element and the XRD analysis results, the black particle phases could be determined as BN. However, the content of black particle phases lessened due to the less added BN content. Besides the N and B elements, several other elements, such as Fe, Cr, and W, were in the particle phase. The reason is that the size of the particle phases was smaller than the diameter of the electron beam of the energy spectrometer, causing the collection range of the elements to exceed the particle size.

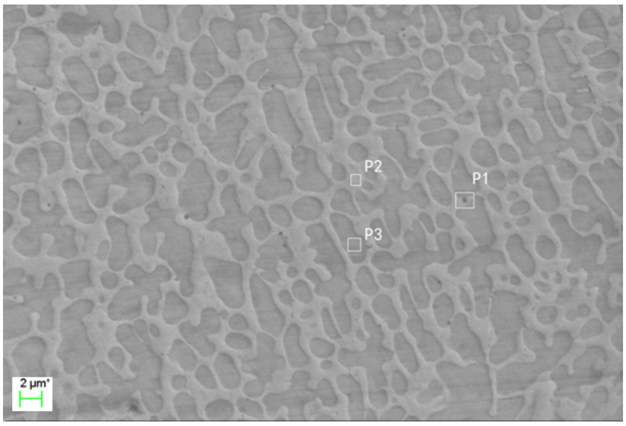


**Fig. 8.** Microstructure of the Ni60A + 24%[WC (80%) + BN] composite coating

**Table 3.** EDS component analysis results for the Ni60A + 24%[WC (80%) + BN] composite coating (mass fraction/%)

| Position | B | C | N | Si | Cr | Fe | Ni | W | Total |
|---|---|---|---|---|---|---|---|---|---|
| articles (P1) | 12.02 | 43.24 | 2.31 | 0.00 | 3.54 | 35.63 | 0.03 | 3.23 | 100 |
| eutectic structure (P2) | 15.79 | 20.35 | 0.03 | 0.00 | 6.42 | 51.82 | 0.11 | 5.49 | 100 |
| dendritic structure (P3) | 24.34 | 12.60 | 0.00 | 0.17 | 3.18 | 58.27 | 0.30 | 1.14 | 100 |

### 4.3.3 Morphology of WC

The physical and chemical properties of WC play an important role in coating performance. If the content of WC phase is too little, the enhancement effect on the cladding layer is not obvious. If the content of WC phase is too much, dendrites tend to appear in the cooling process and cracks tend to appear in the cladding layer. According to the above analysis of phase and energy spectrum, in this study found that WC decomposed. The containing W phases mainly consisted of $Cr_4Ni_{15}W$, $Ni_{17}W_3$, $Fe_7W_6$, and $W_2B$. These W compounds are mainly distributed in the interdendritic eutectic structure and less distributed in the dendritic structure because after the decomposition of WC, it first contacts with fully Ni60A composite powder to generate stable phase and then combines with diffused elements, such as Fe. Thus, the content of W element in the eutectic structure is generally higher than that in the dendrite structure. The sizes of WC particles used in the experiments were large, ranging from 45 μm to 100 μm and from 150 μm to 250 μm [30,31]. Therefore, the WC phase could be detected. In the present study, the reasons for the decomposition of WC in the laser cladding process may be as follows: (1) the WC powder is too fine and the contact between the powders is very sufficient, which provides sufficient conditions for the decomposition of WC powder; and (2) the BN powder is added to the composite powder to produce a catalyst-like effect, which leads to the decomposition of WC.

#### 4.3.4 Morphology and distribution of BN

The physical and chemical properties of BN phase play an important role in coating properties, but its morphology and distribution are equally important. If the content of BN phase is too little, the enhancement and lubrication effect of the composite coating is not obvious. If the content of BN phase is too much, the hardness of the coating decreases seriously. Moreover, the self-lubrication of BN phase no more improved when its content reaches a certain degree. The microstructures of the cladding layer at the top, middle, and bottom parts are shown in Figs. 9(a)–9(c), respectively. Several black particles were distributed on the gray interdendritic eutectic organization. BN phase occasionally appeared, and its distribution was uniform in the dendrite structure of the substrate. As known, the interdendritic eutectic organization was mainly composed of the raw powder. BN was a direct joined phase, and it did not react with other cladding materials. In the process of laser cladding, the other cladding materials could enter the dendrite structure with the form of atoms, which increased the difficulty of BN entering the dendrite structure. However, BN phase dispersion was very uniform on the whole, conducive to the improvement of wear resistance.

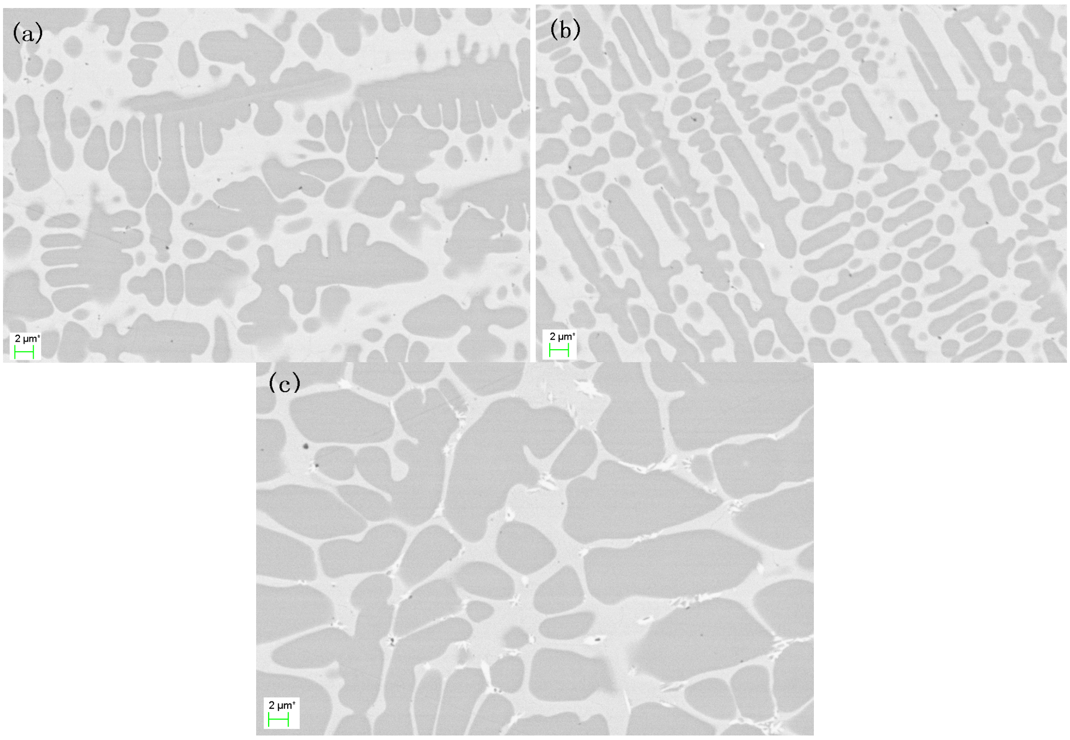


(a) Top of composite coating. (b) Middle of composite coating. (c) Bottom of composite coating

**Fig. 9.** Microstructure of different parts of the Ni60A + 48%[WC (80%) + BN] composite coating

#### 4.3.5 Influence of the composition content on the microstructure

In accordance with the principle of single variable method, the influence of composition contents on the microstructure of cladding layer was explored. Laser cladding samples with different composition contents ratio of composite powder were prepared at the laser power of 1000 W and the scanning speed of 120 mm/min. Fig. 10 shows the microstructure of the cladding layer with different composition contents. The middle part of the cladding layer was observed by SEM, which revealed that the microstructures of the cladding layer consisted of three phases, namely, the dendrites, the eutectic microstructure, and the BN particles. The coarse dendrites gradually became smaller and disorderly as the (WC + BN) content was increased. In view of the content decline of the self-melting Ni60A alloy, the melting point of the composite powder increased as the (WC + BN) content increased. As the melting point increased at the same laser power, the absorbed energy was reduced, the melting degree of the powder decreased, and the undercool degree increased, resulting in a grain nucleation rate higher than the grain growth rate. Thus, fine grains appeared. The distribution of dendrites became disordered due to the irregular direction of the heat dissipation.

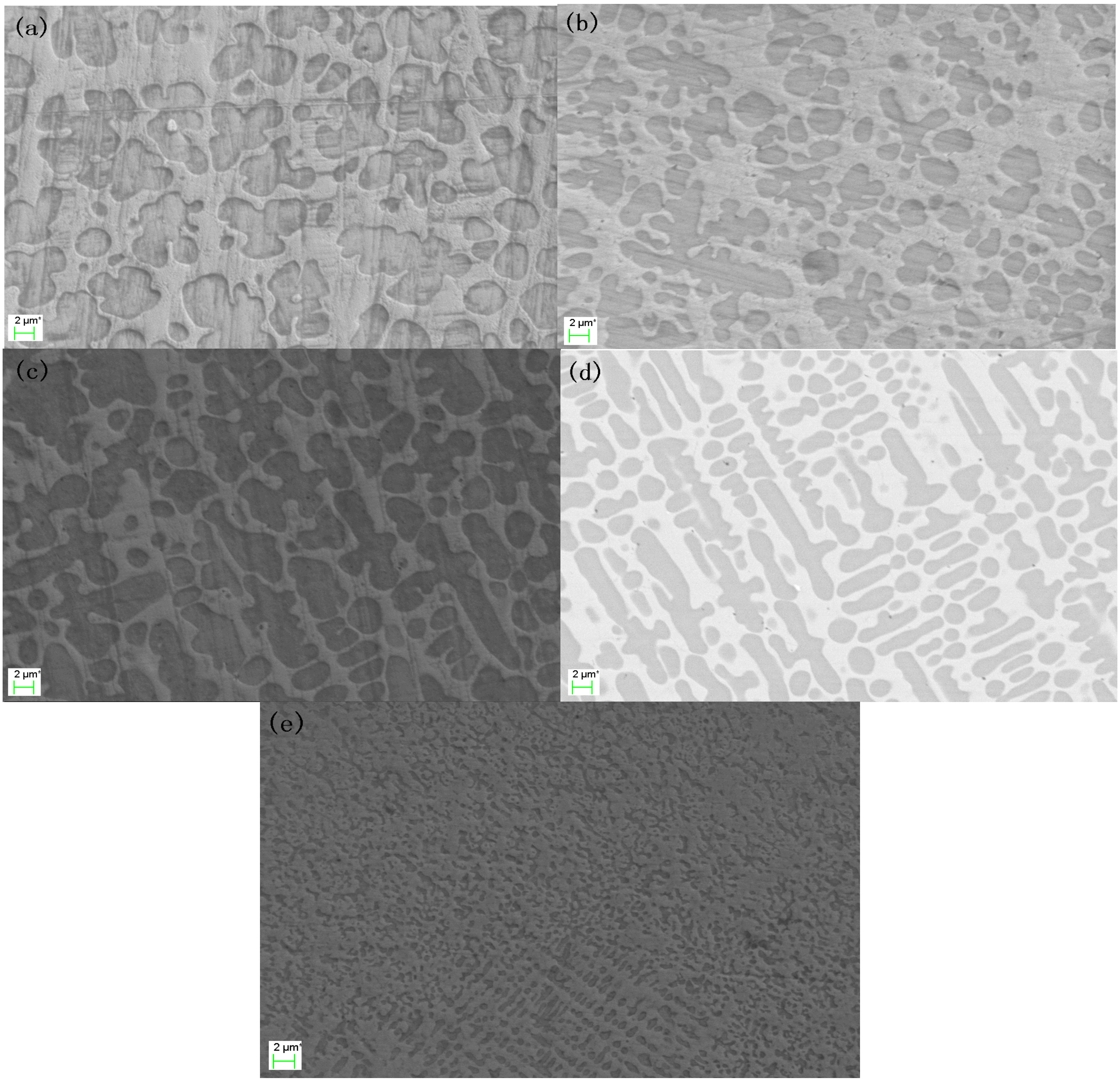

(a) Ni60A + 12%[WC (80%) + BN]. (b) Ni60A + 24%[WC (80%) + BN].
(c) Ni60A + 36%[WC (80%) + BN]. (d) Ni60A + 48%[WC (80%) + BN]. (e) Ni60A + 60%[WC (80%) + BN]

**Fig. 10**. Microstructure of cladding layers of different cladding materials

## 5. Conclusions

The laser cladding parameters, microstructure, and phase composition were comprehensively analyzed to study the reinforcement of Ni-based with WC + BN composite powder on a steel surface by laser cladding. The notable conclusions of this work are as follows:

(1) The cladding composite coating with Ni60A + x%[x%(WC + BN)] composite powder as the raw material was produced on 45 steel surface by laser cladding. The main phases of the cladding composite coating were the Ni-Cr-Fe solid solution, the intermetallic compound $Cr_{23}C_6$, the eutectic compounds $Cr_{22.23}Fe_{0.77}C_6$, and the W compounds. The steel surface could be reinforced using the composite powder of Ni60A + x%[x%(WC + BN)] as the raw material.

(2) Laser power significantly affected the macroscopic morphology and hardness of the cladding layer. At a constant of powder composition ratio, the hardness of cladding layer increased first and then decreased with the increase in laser power, and the maximum hardness appeared at 800 W. In the range of scanning speed set, scanning speed showed obvious influence on hardness of the cladding layer. The hardness of the cladding layer increased with the increase in (WC + BN) content and reached the maximum value of 1262.6 HV1 when the (WC + BN) content was 60%.

(3) Part of WC in the cladding layer was decomposed. BN phase was uniformly distributed in fine and round granular form, mainly distributed in the interdendritic eutectic structure of the cladding coating. With the increase in (WC + BN) content, the number of W-containing compounds and BN particles increased obviously, which is beneficial to improve the hardness and wear resistance of the material.

This study proposed the method of laser cladding of Ni-based Ni60A + x%[x%(WC + BN)] composite powder on 45 steel surface to form reinforced coating and proved the feasibility of this method. The process parameters of laser power, scanning speed, and composition proportion were determined and optimized. The findings of this study provide guidance to the practical application of laser cladding. However, in this study, only laser power, scanning speed, and composition proportion were studied. Thus, more process parameters should be considered in future studies to further improve the process level and material organization properties.

**Acknowledgements**
This work was supported by the Key Research Project of Henan Province Department of Education (Project No.22B460019).



## References

1. Zhang Zh., Radovan K., "Laser cladding of iron-based erosion resistant metal matrix composites". *Journal of Manufacturing Processes*, 38, 2021, pp. 63-75.
2. Han Ch. Y., Sun Y. N., Xu Y. F., Zhang R. H., Lu Ch., Zhao F., "Research on wear and electrochemical corrosion properties of laser cladding nickel base alloy". *Surface Technology*, 50(11), 2021, pp. 103-110.
3. N. Thawari, C. Gullipalli, J. K. Katiyar, T.V.K. Gupta., "Effect of multi-layer laser cladding of Stellite 6 and Inconel 718 materials on clad geometry, microstructure evolution and mechanical properties". *Materials Today Communications,* 28, 2021, pp. 102604.
4. L. Lizzul, M. Sorgato, R. Bertolini, A. Ghiotti, S. Bruschi, F. Fabbro, S. Rech, "On the influence of laser cladding parameters and number of deposited layers on as-built and machined AISI H13 tool steel multilayered claddings". *CIRP Journal of Manufacturing Science and Technology,* 35, 2021, pp. 361-370.
5. A.Behera, A. K. Sahoo, " Wear behaviour of Ni based superalloy: A review". *Materials Today: Proceedings,* 33, 2020, pp. 5638-5642.
6. S. Konovalov, K. Osintsev, A. Golubeva, V. Smelov, Y. Ivanov, X. Chen, I. Komissarova, "Surface modification of Ti-based alloy by selective laser melting of Ni-based superalloy powder". *Journal of Materials Research and Technology,* 9(4), 2020, pp. 8796-8807.
7. Yao F. P., Fang L. J., Li G. S., "Study on structure and process performance of laser cladding nickel-based coating". *Journal of materials research and technology*, 13, 2021, pp. 138-143.
8. M. Oge, A. C. Karaoglanli, M. B. Celik, "Room and high temperature wear behaviors of steelmaking slag coating and WC-reinforced composite coatings". *Surface & Coatings Technology,* 399, 2020, pp. 126162.
9. L. K. Foong, B. H. Jume, C. Y. Xu, "Densification behavior and mechanical properties of hot-pressed TiC–WC ceramics". *Ceramics International,* 46, 2020, pp. 28316-28323.
10. A.A. Zaitsev, A.V. Korotitskiy, E.A. Levashov, E.N. Avdeenko, "Compressive creep of coarse-grain WC-Co and WC-TaC-Co hardmetals with uniform microstructure comprising rounded WC grains". *Materials Science & Engineering A*, 795, 2020, pp. 139998.
11. Yan H., Zhang P. L., Gao Q. Sh., Qin Y., Li R. D., "Laser cladding Ni-based alloy/nano-Ni encapsulated h-BN self-lubricating composite coatings". *Surface & Coatings echnology,* 332, 2017, pp. 422-427.
12. Ankit G., Manowar H., Saurav M., Alok K. D., Amitava M., "Processing and characterization of laser sintered hybrid B4C/cBN reinforced Ti-based metal matrix composite". *Optics and Lasers in Engineering ,*105, 2018, pp.159-172.
13. Debjit M., Vaibhav N., Suman M., Satyajit C., "Effect of hBN and SiC addition on laser assisted processing of ceramic matrix composite coatings". *Ceramics International,* 46, 2020. pp. 9758-9764.
14. Zhao Y., Feng K., Yao Ch. W., Nie P. L., Huang J., Li Zh. G., "Microstructure and tribological properties of laser cladded self-lubricating nickel-base composite coatings containing nano-Cu and h-BN solid lubricants". *Surface & Coatings Technology,* 359, 2019, pp. 485-494.
15. M. Erfanmanesh, R. Shoja-Razavi, H. Abdollah-Pour, H. Mohammadian-Semnani, M. Barekat, S. H. Hashemi., "Friction and wear behavior of laser cladded WC-Co and Ni/WC-Co deposits at high temperature". *International Journal of Refractory Metals & Hard Materials*, 81, 2019, pp. 137-148.
16. Zhu H. M., Mengna O., Hu J. P., Zhang J. W., Qiu Ch. J., "Design and development of TiC-reinforced 410 martensitic stainless steel coatings fabricated by laser cladding". *Ceramics International,* 47, 2021, pp.12505-12513.
17. U.O. O., I.O. O., I.D. A., "Dry sliding wear behaviour of binary powder laser cladded Ti-6Al-4V using SiC and Al". *Materials Today: Proceedings,* 38, 2021, pp. 988-993.
18. Guo Y., Zhang Y. Q., Li Zh. Y., Wei Sh. Zh., Zhang T., Yang L. Q., Liu Sh. Y., "Microstructure and properties of in-situ synthesized ZrC-Al3Zr reinforced composite coating on AZ91D magnesium alloy by laser cladding". *Surface & Coatings Technology,* 334, 2018, pp. 471-478.
19. Hu L. W., Liu X., Chen T. X., Le G. M., Li J. F., Qu F. Sh., Zhou Y. Zh., Qi L., Wang D., "Characterization of laser cladded Zr-Cu-Ni-Al in-situ metallic glass matrix composite coatings with enhanced corrosion-resistance". *Vacuum,* 185, 2021, pp. 109996.
20. Chaiane M., Canedaa J. B., Fogagnolo, Claudio S., Kiminami, Conrado R.M. A., "Ultrafine eutectic coatings from Fe-Nb-B powder using laser cladding". *Materials Characterization*, 160, 2020, pp. 110080.
21. Li H.C., Wang D.G., Hu C., Dou J.H., Yu H.J., Chen C.Z., "Effect of Na2O and ZnO on the microstructure and properties of laser cladding derived CaO-SiO2 ceramic coatings on titanium alloys". *Journal of Colloid and Interface Science,* 592, 2021, pp. 498-508.
22. Liu H. F., Su H. J., Shen Zh. L., Zhao D., Liu Y., Guo Y. N., Guo H. T., Guo M., Xie K. Y., Zhang J., Liu L., Fu H. Zh., "One-step additive manufacturing and microstructure evolution of melt-grown Al2O3/GdAlO3/ZrO2 eutectic ceramics by laser directed energy deposition". *Journal of the European Ceramic Society,* 41, 2021, pp. 3547-3558.
23. Qiu Y., Jiang G. Y., "Study on friction, wear and thermal insulation properties of laser deposition Ni/$ZrO_2$". *Optik - International Journal for Light and Electron Optics,* 247, 2021, pp. 167783.
24. Lu J. Z., Cao J., Lu H. F., Zhang L. Y., Luo K.Y., "Wear properties and microstructural analyses of Fe-based coatings with various WC contents on H13 die steel by laser cladding". *Surface & Coatings Technology*, 369 2019, pp. 228-237.
25. B. AlMangour, D. Grzesiak, J. M. Yang, "In-situ formation of novel TiC-particle-reinforced 316L stainless steel bulk-form composites by selective laser melting". *Journal of Alloys and Compounds,* 706, 2017, pp. 409-418.
26. U.O. Okoli, I.O. Otunniyi, I.D. Adebiyi, "Dry sliding wear behaviour of binary powder laser cladded Ti-6Al-4V using SiC and Al". *Materials Today: Proceedings*, 38, 2021, pp. 988-993.
27. Zhang L., Wang C. Sh., Han L. Y., Dong Ch., "Influence of laser power on microstructure and properties of laser clad Co-based amorphous composite coatings". *Surfaces and Interfaces,* 6, 2017, pp. 18-23.
28. Zhao Y., Feng K., Yao Ch. W., Nie P. L., Huang J., Li Zh. G., "Microstructure and tribological properties of laser cladded self-lubricating nickel-base composite coatings containing nano-Cu and h-BN solid lubricants". *Surface & Coatings Technology*, 359, 2019, pp. 485-494.
29. Huang X., Zhang J. Ch., Cheng Y., Chen Ch. R., Lian G. F., Jiang J. B., Feng M. Y., Zhou M. N., "Effect of h-BN addition on the microstructure characteristics, residual stress and tribological behavior of WC-reinforced Ni-based composite coatings". *Surface & Coatings Technology,* 405, 2021, pp. 126534.
30. Liu J. D., Zhang Sh. Q., Wang H. M., "Microstructure and wear resistance of laser cladding WC particles reinforced composite coatings". *The Chinese Journal of Nonferrous Metals,* 22(9), 2012, pp. 2600-2607.
31. Zang Ch. Ch., Wang Y. Zh., Zhang Y. D., Li J. H., Zeng H., Zhang D. Q., "Microstructure and Tribological Behavior of Ni60 +35WC-Ni Coating Produced by Laser Cladding". *Chinese Journal of Rare Metals*, 39(5), 2015, pp. 385-391.